Characterization and modeling of microstructured chalcogenide fibers for efficient mid-infrared wavelength conversion

Sida Xing, Davide Grassani,[*] Svyatoslav Kharitonov, Adrien Billat, and Camille-Sophie Brès

Ecole Polytechnique Fédérale de Lausanne (EPFL), Photonic Systems Laboratory (PHOSL), STI-IEL, Station 11, CH-1015 Lausanne, Switzerland
[*]*davide.grassani@epfl.ch*

Abstract: We experimentally demonstrate wavelength conversion in the 2 μm region by four-wave mixing in an AsSe and a GeAsSe chalcogenide photonic crystal fibers. A maximum conversion efficiency of −25.4 dB is measured for 112 mW of coupled continuous wave pump in a 27 cm long fiber. We estimate the dispersion parameters and the nonlinear refractive indexes of the chalcogenide PCFs, establishing a good agreement with the values expected from simulations. The different fiber geometries and glass compositions are compared in terms of performance, showing that GeAsSe is a more suited candidate for nonlinear optics at 2 μm. Building from the fitted parameters we then propose a new tapered GeAsSe PCF geometry to tailor the waveguide dispersion and lower the zero dispersion wavelength (ZDW) closer to the 2 μm pump wavelength. Numerical simulations shows that the new design allows both an increased conversion efficiency and bandwidth, and the generation of idler waves further in the mid-IR regions, by tuning the pump wavelength in the vicinity of the fiber ZDW.

OCIS codes: (190.4380) Nonlinear optics, four-wave mixing; (190.4370) Nonlinear optics, fibers; (060.2390) Fiber optics, infrared; (140.3070) Infrared and far-infrared lasers.

References and links

1. S. Moro, A. Danicic, N. Alic, N. G. Usechak, and S. Radic, "Widely-tunable parametric short-wave infrared transmitter for CO2 trace detection," Opt. Express **19**(9), 8173–8178 (2011).
2. J. Lesh, "Free space laser communications," in *Summaries of Papers Presented at the Conference on Lasers and Electro-Optics, 1999* (IEEE, 1999), pp. 316.
3. C. Weitkamp, *Lidar: Range-Resolved Optical Remote Sensing of the Atmosphere*, vol. 102 (Springer, 2006).
4. R. R. Anderson, W. Farinelli, H. Laubach, D. Manstein, A. N. Yaroslavsky, J. Gubeli 3rd, K. Jordan, G. R. Neil, M. Shinn, W. Chandler, G. P. Williams, S. V. Benson, D. R. Douglas, and H. F. Dylla, "Selective photothermolysis of lipid-rich tissues: A free electron laser study," Lasers Surg. Med. **38**(10), 913–919 (2006).
5. G. Edwards, R. Logan, M. Copeland, L. Reinisch, J. Davidson, B. Johnson, R. Maciunas, M. Mendenhall, R. Ossoff, J. Tribble, J. Werkhaven, and D. O'Day, "Tissue ablation by a free-electron laser tuned to the amide II band," Nature **371**(6496), 416–419 (1994).
6. T. Torounidis and P. Andrekson, "Broadband single-pumped fiber-optic parametric amplifiers," IEEE Photonics Technol. Lett. **19**(9), 650–652 (2007).
7. B. Kuyken, X. Liu, G. Roelkens, R. Baets, R. M. Osgood, Jr., and W. M. Green, "50 dB parametric on-chip gain in silicon photonic wires," Opt. Lett. **36**(22), 4401–4403 (2011).
8. S. Zlatanovic, J. S. Park, S. Moro, J. M. C. Boggio, I. B. Divliansky, N. Alic, S. Mookherjea, and S. Radic, "Mid-infrared wavelength conversion in silicon waveguides using ultracompact telecom-band-derived pump source," Nat. Photonics **4**(8), 561–564 (2010).
9. B. Kuyken, P. Verheyen, P. Tannouri, X. Liu, J. Van Campenhout, R. Baets, W. M. Green, and G. Roelkens, "Generation of 3.6 μm radiation and telecom-band amplification by four-wave mixing in a silicon waveguide with normal group velocity dispersion," Opt. Lett. **39**(6), 1349–1352 (2014).
10. R. K. Lau, M. Ménard, Y. Okawachi, M. A. Foster, A. C. Turner-Foster, R. Salem, M. Lipson, and A. L. Gaeta, "Continuous-wave mid-infrared frequency conversion in silicon nanowaveguides," Opt. Lett. **36**(7), 1263–1265 (2011).

#259937 Received 26 Feb 2016; revised 30 Mar 2016; accepted 31 Mar 2016; published 26 Apr 2016

11. S. Zlatanovic, J. S. Park, S. Moro, J. M. C. Boggio, I. B. Divliansky, N. Alic, S. Mookherjea, and S. Radic, "Mid-infrared wavelength conversion in silicon waveguides using ultracompact telecom-band-derived pump source," Nat. Photonics **4**(8), 561–564 (2010).
12. X. Liu, B. Kuyken, G. Roelkens, R. Baets, R. M. Osgood, Jr., and W. M. Green, "Bridging the mid-infrared-to-telecom gap with silicon nanophotonic spectral translation," Nat. Photonics **6**(10), 667–671 (2012).
13. C.-S. Brès, S. Zlatanovic, A. O. Wiberg, and S. Radic, "Continuous-wave four-wave mixing in cm-long Chalcogenide microstructured fiber," Opt. Express **19**(26), B621–B627 (2011).
14. S. D. Le, D. M. Nguyen, M. Thual, L. Bramerie, M. Costa e Silva, K. Lenglé, M. Gay, T. Chartier, L. Brilland, D. Méchin, P. Toupin, and J. Troles, "Efficient four-wave mixing in an ultra-highly nonlinear suspended-core chalcogenide As38Se62 fiber," Opt. Express **19**(26), B653–B660 (2011).
15. R. E. Slusher, G. Lenz, J. Hodelin, J. Sanghera, L. B. Shaw, and I. D. Aggarwal, "Large Raman gain and nonlinear phase shifts in high-purity As 2 Se 3 chalcogenide fibers," J. Opt. Soc. Am. B **21**(6), 1146–1155 (2004).
16. J. Troles, Q. Coulombier, G. Canat, M. Duhant, W. Renard, P. Toupin, L. Calvez, G. Renversez, F. Smektala, M. El Amraoui, J. L. Adam, T. Chartier, D. Mechin, and L. Brilland, "Low loss microstructured chalcogenide fibers for large non linear effects at 1995 nm," Opt. Express **18**(25), 26647–26654 (2010).
17. are I. Savelli, O. Mouawad, J. Fatome, B. Kibler, F. Désévédavy, G. Gadret, J.-C. Jules, P.-Y. Bony, H. Kawashima, W. Gao, T. Kohoutek, T. Suzuki, Y. Ohishi, and F. Smektala, "Mid-infrared 2000-nm bandwidth supercontinuum generation in suspended-core microstructured Sulfide and Tellurite optical fibers," Opt. Express **20**(24), 27083–27093 (2012).
18. Y. Yu, B. Zhang, X. Gai, C. Zhai, S. Qi, W. Guo, Z. Yang, R. Wang, D.-Y. Choi, S. Madden, and B. Luther-Davies, "1.8-10 μm mid-infrared supercontinuum generated in a step-index chalcogenide fiber using low peak pump power," Opt. Lett. **40**(6), 1081–1084 (2015).
19. T. Cheng, L. Zhang, X. Xue, D. Deng, T. Suzuki, and Y. Ohishi, "Broadband cascaded four-wave mixing and supercontinuum generation in a tellurite microstructured optical fiber pumped at 2 μm," Opt. Express **23**(4), 4125–4134 (2015).
20. D. Grassani, S. Xing, S. Kharitonov, A. Billat, S. Cordette, A. Vedadi, and C.-S. Brès, "Continuous wave four-wave mixing at 2 micron in Chalcogenide microstructured fiber," in *Advanced Solid State Lasers* (Optical Society of America, 2015), paper ATu3A. 6.
21. G. Agrawal, "Chapter 10 - Four-Wave Mixing," in *Nonlinear Fiber Optics (Fifth Edition)*, G. Agrawal, ed. (Academic, 2013), pp. 397–456.
22. N. Shibata, R. P. Braun, and R. G. Waarts, "Phase-mismatch dependence of efficiency of wave generation through four-wave mixing in a single-mode optical fiber," IEEE J. Quantum Electron. **23**(7), 1205–1210 (1987).
23. S. Kharitonov, A. Billat, L. Zulliger, S. Cordette, A. Vedadi, and C.-S. Brès, "Kerr nonlinearity of Thulium-doped fiber near 2 μm," in *CLEO: Science and Innovations* (Optical Society of America, 2015), paper JTu5A. 31.
24. M. J. Steel, T. P. White, C. Martijn de Sterke, R. C. McPhedran, and L. C. Botten, "Symmetry and degeneracy in microstructured optical fibers," Opt. Lett. **26**(8), 488–490 (2001).
25. O. Mouawad, F. Amrani, B. Kibler, J. Picot-Clémente, C. Strutynski, J. Fatome, F. Désévédavy, G. Gadret, J. C. Jules, O. Heintz, E. Lesniewska, and F. Smektala, "Impact of optical and structural aging in As_2S_3 microstructured optical fibers on mid-infrared supercontinuum generation," Opt. Express **22**(20), 23912–23919 (2014).
26. G. Lenz, J. Zimmermann, T. Katsufuji, M. E. Lines, H. Y. Hwang, S. Spälter, R. E. Slusher, S.-W. Cheong, J. S. Sanghera, and I. D. Aggarwal, "Large Kerr effect in bulk Se-based chalcogenide glasses," Opt. Lett. **25**(4), 254–256 (2000).
27. J. Fatome, C. Fortier, T. Chartier, F. Smektala, K. Messaad, B. Kibler, S. Pitois, G. Gadret, C. Finot, J. Troles, F. Desevedavy, P. Houizot, G. Renversez, L. Brilland, and N. Traynor, "Linear and nonlinear characterizations of chalcogenide photonic crystal fibers," J. Lightwave Technol. **27**(11), 1707–1715 (2009).
28. P. Toupin, L. Brilland, J. Trolès, and J.-L. Adam, "Small core Ge-As-Se microstructured optical fiber with single-mode propagation and low optical losses," Opt. Mater. Express **2**(10), 1359–1366 (2012).
29. H. G. Dantanarayana, N. Abdel-Moneim, Z. Tang, L. Sojka, S. Sujecki, D. Furniss, A. B. Seddon, I. Kubat, O. Bang, and T. M. Benson, "Refractive index dispersion of chalcogenide glasses for ultra-high numerical-aperture fiber for mid-infrared supercontinuum generation," Opt. Mater. Express **4**(7), 1444–1455 (2014).
30. P. Ma, D.-Y. Choi, Y. Yu, X. Gai, Z. Yang, S. Debbarma, S. Madden, and B. Luther-Davies, "Low-loss chalcogenide waveguides for chemical sensing in the mid-infrared," Opt. Express **21**(24), 29927–29937 (2013).
31. P. S. J. Russell, "Photonic-crystal fibers," J. Lightwave Technol. **24**(12), 4729–4749 (2006).
32. S. D. Le, M. Gay, L. Bramerie, M. Costa e Silva, K. Lenglé, T. Chartier, M. Thual, J.-C. Simon, L. Brilland, D. Méchin, P. Toupin, and J. Troles, "Wavelength conversion in a highly nonlinear chalcogenide microstructured fiber," Opt. Lett. **37**(22), 4576–4578 (2012).

1. Introduction

The Short-Wave (SWIR) (1400-2500 nm) and the Mid-Infrared (MIR) regions are receiving a growing amount of attention due to the large number of potential applications that can be developed in these wavelength ranges. Different gases and pollutants have strong molecular

#259937 Received 26 Feb 2016; revised 30 Mar 2016; accepted 31 Mar 2016; published 26 Apr 2016

fingerprint in the 2 μm range [1], making it attractive for sensing and spectroscopy. The atmospheric transparency in the 2 - 2.5 μm window enables secure optical free-space communication systems, remote sensing and LIDAR techniques [1–3]. Because of distinctive tissue absorption at these wavelengths, non-invasive medical diagnostic and novel laser surgery are other promising applications [4, 5]. Moreover, 2 μm laser sources can be used for pumping nonlinear media to achieve all-optical ultrafast processing and generate light at targeted wavelengths deeper into the MIR through four-wave mixing (FWM).

FWM with high gain and large bandwidth has been achieved in silica highly nonlinear fibers with pumping in the telecommunication band [6]. However silica suffers from excessive losses beyond 2 μm and novel materials, with strong optical nonlinearity and high transparency over a broad wavelength range, have to be considered for processing in the SWIR and MIR. Silicon, showing reduced two photon absorption, large Kerr nonlinearity and high refractive index at 2 μm, is a potential candidate. Dispersion engineered silicon integrated waveguides with strong light confinement have been successfully employed to achieve optical parametric amplification [7, 8], wavelength conversion [7–11], and bi-directional broadband spectral translation of optical signals [12].

An alternative approach relies on using chalcogenide glass (ChG) microstructured fibers as nonlinear medium. In fact, chalcogenide glasses have a very wide transparency windows up to 10 μm or 15 μm in the MIR, depending on the glass composition, and a very high third order nonlinearity, up to 1000 times the one of silica. In addition, through control of their geometry, microstructured fibers offer a lot of freedom in terms of dispersion engineering, an essential ingredient to achieve phase matching for efficient FWM. Finally, as chalcogenide glasses can be drawn in fibers and owing to the recent progress in fabrication techniques, long interaction length and very low propagation losses can be relied upon. Demonstration of FWM and Raman gain in the telecom band has already been shown in [13–15], together with Raman scattering at 2 μm [16] and supercontinuum generation in the MIR [17–19]. Recently we observed preliminary results on FWM at 2 μm in an AsSe PCF [20].

Here we report the quantitative study of nonlinear parameter and dispersion properties of chalcogenide microstructured fibers by FWM at 2 μm. Moreover, we use a continuous wave (CW) pump which is suitable for applications such as precise spectroscopy or communication. We tested two fibers with different geometry and composition. The first fiber-under-test (FUT1) is an AsSe photonic crystal fiber with a core diameter of 14 μm and zero dispersion wavelength (ZDW) at about 5.1 μm. The second fiber-under-test (FUT2) is a GeAsSe photonic crystal fiber, with a small core diameter of 4 μm and a blue-shifted ZDW at about 3 μm. We experimentally reconstruct the conversion bandwidth of the two fibers and estimate their dispersion parameters and their nonlinear coefficients. Comparing these values with numerical simulations we derive the Kerr index of the two materials in the 2 μm wavelength region. Finally, based on our extracted parameters, we propose a new design for blue shifting the ZDW: a tapered GeAsSe PCF. We perform numerical simulations showing a potential solution for increasing conversion efficiency and extending the conversion bandwidth further into the SWIR and MIR regions.

2. FWM in ChG PCF

Four-wave-mixing is a third order nonlinear process in which two pump photons at frequency ω_{p1}, ω_{p2} interact to generate a signal photon at ω_s and an idler photon at ω_i conserving both energy and momentum. In wavelength conversion experiments, the two pump photons are usually degenerate ($\omega_{p1} = \omega_{p2} = \omega_p$) in frequency and the process is stimulated by a signal seed which adds a constrain on the energy conservation, limiting the generated idler frequency to: $\omega_i = 2\omega_p - \omega_s$. In optical fibers, the momentum conservation is given by the phase matching between the pump, signal and idler waves. Considering both linear and nonlinear contribution, the phase mismatch is [21]:

#259937 Received 26 Feb 2016; revised 30 Mar 2016; accepted 31 Mar 2016; published 26 Apr 2016

$$\Delta k + 2\gamma P \approx \beta_2 \Delta\omega^2 + \frac{1}{12}\beta_4 \Delta\omega^4 + 2\gamma P = 0. \quad (1)$$

In the previous equation, Δk is the linear phase mismatch, β_2 and β_4 are the second and fourth order derivatives of the mode propagation constant, $\Delta\omega$ is the signal detuning from the pump angular frequency, while γ and P are the fiber's nonlinear coefficient and the coupled pump power, respectively. A useful parameter to characterize nonlinear media is the conversion efficiency (CE), defined as the ratio of the generated idler power over the injected signal power. In highly dispersive materials like ChG, considering typical coupled powers of tens of mW in CW regime, we can safely neglect the nonlinear contribution to the phase mismatch and the CE can be written as [22]:

$$CE = \frac{P_i}{P_s} = \varepsilon \left(\gamma P_p\right)^2 \left(\frac{1 - e^{-\alpha L}}{\alpha}\right)^2 \quad (2)$$

where

$$\varepsilon = \frac{\alpha^2}{\alpha^2 + \Delta k^2}\left(\frac{4e^{-\alpha L}\sin^2(\Delta k L/2)}{(1 - 4\,\mathrm{e}^{-\alpha \mathrm{L}})^2}\right) \quad (3)$$

in Eqs. (2) and (3), α represents the linear losses, and L the length of the fiber. From Eqs. (2) and (3) it results that, from the measured FWM spectra, as a function of signal wavelength and pump power it is possible to retrieve dispersion and nonlinearity of the fiber.

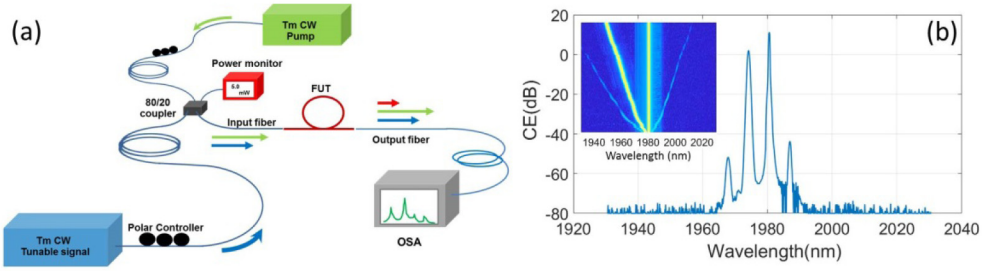

Fig. 1. (a) Experimental set-up for FWM measurement. (b) An example of FWM spectrum taken at a pump power of 54 mW and signal power of about 6 mW. The inset shows a colormap of idler generation at the Stokes and anti-Stokes sides for the pump at 1981 nm and swept signal from 1950 nm to 1978 nm.

In order to assess the dispersion and the nonlinear optical properties of the FUTs, we used the experimental setup shown in Fig. 1(a). Two custom made polarized tunable Thulium (Tm) doped CW fiber lasers [23] were used as pump and signal. The pump laser is based on a ring cavity design embedding a 4 m long Thulium doped fiber pumped at 1600 nm and a fixed 0.5 nm wide fiber Bragg grating at 1981 nm or 2008 nm. The obtained pump linewidth is about 0.2 nm. The signal laser is also a ring cavity with 11.5 m Thulium doped fiber double-side pumped at 1600 nm and a tunable grating filter (2 nm wide), leading to a laser linewidth of 0.4 nm. The signal tunable range is approximately 100 nm centered at 2000 nm, limited by the tunable grating filter. Polarization controllers on the pump and signal lasers are added to align the polarization states. It is important to notice that changing the pump polarization state does not give any significant change in the conversion efficiency and bandwidth, once the signal polarization is always aligned along the pump one. This means that no birefringence is observed in the samples, as expected from hexagonal structures [24]. Pump and signal are then combined by a 50/50 coupler, and sent to the fiber under test (FUT). We employed a

#259937 Received 26 Feb 2016; revised 30 Mar 2016; accepted 31 Mar 2016; published 26 Apr 2016

butt-coupling technique using a cleaved single mode fiber (SMF-28) to inject light into FUT1, and a standard silica multi-mode fiber with a core diameter of 50 µm to collect the transmitted light. Two identical polarization maintaining Nufern PM1950 fiber with tapered tip on one end, beam diameter of 4 um at 1950 nm of wavelength, and 11 µm working distance are employed both for in-coupling and out-coupling for FUT2. The maximum input power that can be injected before damaging the fiber is related to different factors, notably: the fiber facet's roughness, input misalignment due to radiation pressure and the melting point of the chalcogenide glass. In our experiment, we were limited mainly by the first two factors and, by accurate polishing of the fiber facets, we could safely inject more than 150 mW in CW in both fibers. Moreover, we did not notice any sign of degradation of the conversion efficiency and bandwidth during the experiments. In fact, water absorption in chalcogenide glasses, due to the exposure to normal atmosphere, mainly affects the quality of the outer surface of the fibers, while the mode is mainly confined inside the core region. In this way we do not need to seal the fiber in special protected atmosphere boxes during the experiment. Light collected from the output fibers is then sent to an optical spectrum analyzer (OSA) for analysis. Figure 1(b) shows an example of the optical spectrum placing the signal laser on the Stokes side of the pump wavelength in the FUT1. The inset of Fig.1(b) shows idlers generated on both Stokes and anti-Stokes sides of the pump, due to the strong nonlinearity of the medium and the relatively high signal power, while multiple periods of oscillations are observed due to the high dispersion of the fiber at 2 µm.

3. Experimental results

3.1 FUT1

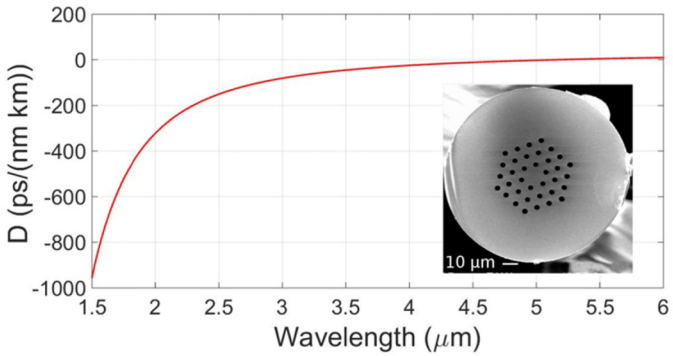

Fig. 2. Dispersion parameter as a function of the wavelength for FUT1. Inset: SEM image of the cross section of the FUT1.

The material composition of FUT1 is $As_{38}Se_{62}$, and the fiber length is 31.5 cm. A scanning electron microscope (SEM) of the fiber cross-section (Fig. 2 inset), is used to get a precise measurement of its geometry. The core diameter is 14 µm while the external diameter is 125 µm. The air hole diameter d and the pitch distance Λ are measured to be about 3.79 µm and 8.54 µm, respectively. This gives a diameter to pitch ratio r = d/Λ of 0.44 between air hole diameter and pitch distance, leading to a single mode behavior of the fiber in the 2 micron wavelength region. We performed numerical simulations with a finite element method (FEM) based software to compute the fiber dispersion over the wavelength range from 1.5 µm to 6 µm (Fig. 2). We used the measured geometrical parameter of the fiber cross section and we interpolated the measured refractive index values of the bulk glass given by the manufacturer to retrieve an analytical formula for the AsSe PCF dispersion. As expected, due to the large core diameter compared to the operating wavelength, the overall dispersion is dominated by the material dispersion, such that the zero dispersion wavelength (ZDW) is at about 5.1 µm.

#259937 Received 26 Feb 2016; revised 30 Mar 2016; accepted 31 Mar 2016; published 26 Apr 2016

As a first step, we characterized idler generation as a function of pump power for a fixed signal wavelength at 6 nm of detuning from the pump placed at 1981 nm. The total losses, measured between the input of the SM input fiber to the output of the MM fiber are 11 dB, while linear losses, estimated by cut-back to be between 4.5 and 6 dB/m, are slightly higher than the nominal value. Higher linear losses are attributed to water absorption, aging and photodarkening [25]. As expected, the CE as a function of the pump power follows a quadratic behavior, as it is shown in Fig. 3(a). Maximum CE of about −36 dB is registered without any sign of saturation. In Fig. 3(b) we vary the signal power keeping the pump power constant, verifying a linear dependence between idler and signal powers. The CE as a function of the wavelength for three different coupled pump powers is shown in Fig. 3(c).

Idler waves are seen over a bandwidth of at least 25 nm with a 3 dB conversion bandwidth of about 18 nm considering both sides of the pump. As seen in Fig. 3(c), the conversion bandwidth does not change as a function of the pump power, confirming our assumption that the nonlinear contribution to the phase mismatch can be neglected. In Fig. 3(d) we normalize the three curves to the coupled pump power squared and fit the data with the normalized Eq. (2) to retrieve the dispersion parameter $D = -2\pi c\beta_2/\lambda^2$ and the nonlinear coefficient γ. We used different fitting curves, with different α values ranging from 4.5 dB/m to 6 dB/m. The estimated dispersion is $D = -336$ ps/nm/km, in good agreement with the value ($D = -334$ ps/nm/km) reported in Fig. 2, while the average nonlinear parameter is $\gamma = 0.53$ $W^{-1}m^{-1}$. In order to compare the retrieved nonlinearity with those already published in literature, we derived the nonlinear refractive index n_2 from the estimated γ and the mode effective area of the fiber (A_{eff}) obtained from FEM simulations: $n_2 = \lambda A_{eff}\gamma/2\pi \approx 7.9\cdot10^{-14}$ cm^2/W. This value is indeed consistent with previous results found in literature at telecommunication wavelength obtained by z-scan experiment: $n_2 \approx 1.1\cdot10^{-13}$ cm^2/W [26], self-phase modulation $n_2 \approx 1.1\cdot10^{-13}$ cm^2/W [27] and by four wave mixing: $n_2 \approx 1.3\cdot10^{-13}$ cm^2/W [14].

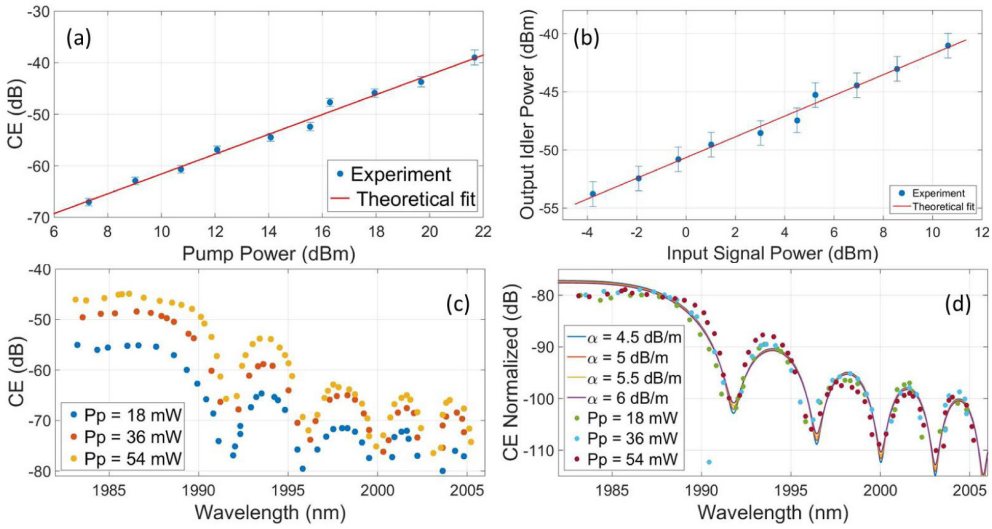

Fig. 3. (a) CE as a function of coupled pump power and theoretical fit of a quadratic polynomial. (b) Idler output power as a function of the signal input power for a coupled pump power of 16 dBm and theoretical fit of a linear polynomial. Error bars are calculated by standard error propagation considering uncertainty on pump and signal lasers of 0.5 dB. (c) CE as a function of generated idler wavelength for three coupled pump powers. (d) CE for three coupled pump powers normalized to pump power squared and superimposed to the theoretical CE/P_p^2 plotted with different linear losses values.

#259937 Received 26 Feb 2016; revised 30 Mar 2016; accepted 31 Mar 2016; published 26 Apr 2016

3.2 FUT2

The data analysis on the FUT1 reveals that, despite the high Kerr index of AsSe glass, the efficiency of the FWM process at 2 µm is still limited by the large phase mismatch between pump, signal and idler, and by the large A_{eff} which lowers the nonlinear coefficient. Diminishing the core size of the PCF allows to simultaneously enhance γ and lower the phase mismatch, thus shifting the ZDW of the fiber towards 2 µm. From a technological point of view, low loss ChG PCF with core diameter smaller than about 5 µm are very difficult to obtain with AsSe glasses [28]. However, it has been shown that inserting a certain amount of germanium in the glass composition allows to draw small core PCF with less than 1 dB/m optical losses around 2.5 µm [29]. Moreover, the material ZDW of GeAsSe glasses is already blue shifted with respect to the AsSe one. The FUT2 is a 27 cm long $Ge_{10}As_{22}Se_{68}$ PCF. From the SEM image shown in the inset of Fig. 4 we estimated the core diameter to be around 4 µm, air hole diameters d of 1.28 µm and a pitch distance Λ of 2.68 µm, leading to a ratio r ≈0.49. Figure 4 shows the simulated dispersion of FUT2 based on the measured geometrical values, and the refractive index dispersion derived in [30] from ellipsometry measurements performed on a $Ge_{11.5}As_{24}Se_{64.5}$ compound. From the simulation, the ZDW of this fiber is expected to be at 3.015 µm, a significant blue shift compared to FUT1.

We tested the fiber for three different pump wavelengths: 1565 nm, 1981 nm and 2008 nm, with measured coupled pump powers of 36 mW, 65 mW and 60 mW respectively. The average overall losses were about 4.5 dB, with an estimated 2.5 dB in-coupling losses, 1.5 dB out-coupling losses and 0.5 dB of propagation losses, i.e α = 2 dB/m. Figures 5(a)-(c) show the CE as a function of the idler wavelength for the three employed pump wavelength. Superimposed to the experimental data are reported the theoretical fitting curves computed from Eq. (2).

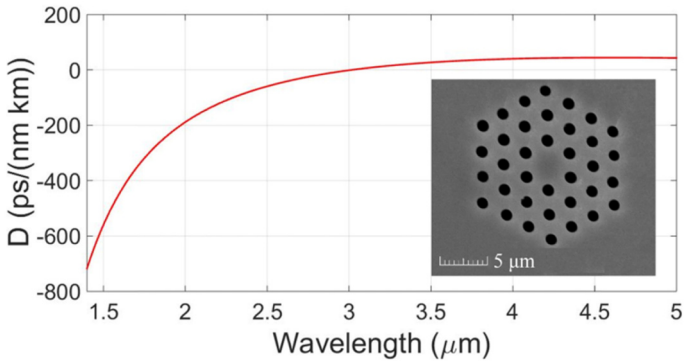

Fig. 4. Dispersion parameter as a function of the wavelength for FUT2. Inset: SEM image of the cross section of the FUT2.

The dispersion parameters are estimated to be D = –171 ps/(nm km) at 2008 nm, D = –183 ps/(nm km) at 1981 nm, and D = –477ps/(nm km) at 1565 nm. As expected, the dispersion decreases in absolute value when the pump wavelength approaches the ZDW, leading to a maximum overall 3 dB conversion bandwidth of 24 nm for the 2008 nm pump wavelength. Comparing the D values retrieved from the fits to the ones of Fig. 4, we notice that the theoretical values D = –185 ps/(nm km), D = –196 ps/(nm km) and D = –480 ps/(nm km) at 2008 nm, 1981 nm and 1565 nm respectively, are slightly larger (in absolute value) than experimental ones, most probably due to small discrepancies in refractive index we used. The trend is however similar.

#259937 Received 26 Feb 2016; revised 30 Mar 2016; accepted 31 Mar 2016; published 26 Apr 2016

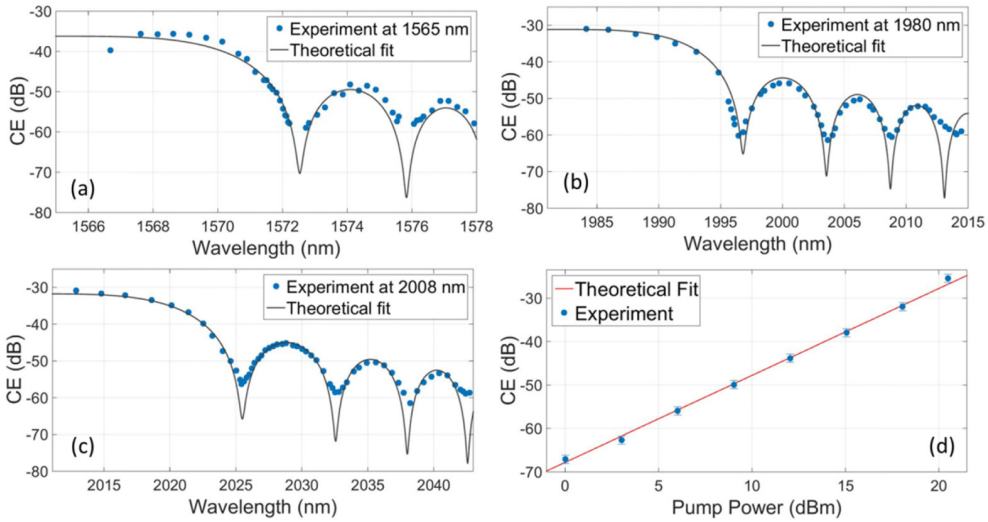

Fig. 5. Experimental CE superimposed to theoretical fits as a function of idler wavelength for pump at (a) 1565 nm, (b) 1981 nm and (c) 2008 nm. (d) CE as a function of the coupled pump power for 1981 nm pump and pump-signal detuning of 6 nm. Error bars are calculated considering 0.5 dB uncertainty on the input lasers power. The red curve is the theoretical fit.

In Fig. 5(d) is shown the CE as a function of the coupled pump power for the 1981 nm pump wavelength, and signal – pump detuning of 6 nm. The experimental data follow very well the expected quadratic dependence, notably there is once again no sign of saturation due to fiber damage or multiphoton absorption and a CE as high as –25.4 dB for a CW coupled pump power of about 20.5 dBm is reported. Comparing this result with the one reported in Fig. 3(b) for FUT1, more than 10 dB increase in the CE per unit length and coupled pump power is observed in the FUT2. Experimental data in Fig. 5(d) are fitted using the dispersion value retrieved from the experiment and setting γ as the fitting parameter. The nonlinear parameter is thus found to be 1.688 ± 0.11 $W^{-1}m^{-1}$. Using the A_{eff} computed from numerical simulations, we estimate the nonlinear refractive index at $n_2 \approx 5.3 \cdot 10^{-14}$ cm^2/W. It should be noted that this is the first estimation of the Kerr index of GeAsSe in the SWIR region.

4. Blue-shift of the ZDW in the 2 µm region

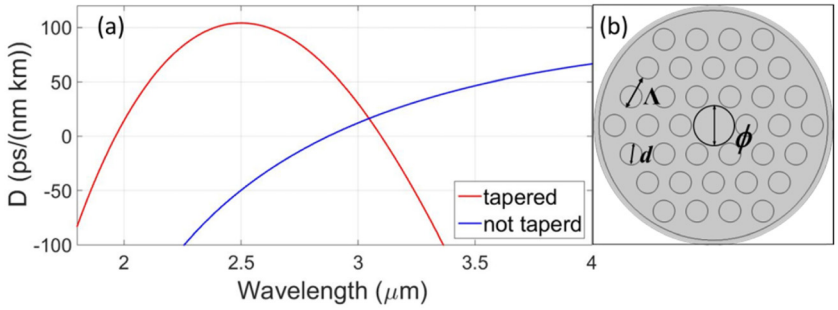

Fig. 6. (a) Dispersion of the r = 0.66 with 4 µm core diameter (red) and the corresponding tapered fiber, with a core diameter of 1.5 µm (blue). (b) Structure of the tapered PCF under simulation.

Despite the improved efficiency, the dispersion of FUT2 in the 2 µm region is still too large and should be compensated by stronger waveguide dispersion. The ZDW of a PCF is highly dependent on the diameter-to-pitch ratio $r = d/\Lambda$ [31], however, larger diameter-to-pitch ratio

#259937 Received 26 Feb 2016; revised 30 Mar 2016; accepted 31 Mar 2016; published 26 Apr 2016

would also increase the fabrication difficulty, especially for soft glasses like ChG PCFs. We performed numerical analysis to blue-shift the ZDW of the GeAsSe PCF and preliminary results showed that varying this ratio alone, within a realistic upper limit of r = 0.7, is not sufficient to shift the ZDW down to 2 μm. At this purpose, a further reduction of the core size diameter ϕ is needed, implying a further technological step for tapering the fiber. While tapering is not a trivial process, low loss tapered three-ring structure GeAsSe PCFs have recently been successfully fabricated [32], showing good uniformity and performance. Tapered fibers were primarily investigated for the purpose of increasing the nonlinearity through a reduction of the effective area. In our design we thus combine high ratio and a small fiber core diameter for dispersion management. The proposed fiber geometry is shown in the inset of Fig. 6. The core is defined as the circle tangential to the first ring of air-holes. From a simple geometry analysis, the fiber core diameter ϕ is found to be:

$$\phi = (2\Lambda - d)T = \left(\frac{2}{r} - 1\right)dT \tag{4}$$

Here, T is the scaling/tapering factor for simulating the tapering process. We assume that the ChG PCF core diameter can be tapered down to 1.5 μm with a good uniformity. In Fig. 6 we show that, using a ratio r = 0.66, the ZDW can be successfully shifted down to 1963.4 nm, in the maximum emission region of Tm doped fiber lasers. In comparison, the ZDW for the corresponding un-tapered geometry is at 2.868 μm. In Fig. 7 the CE of the r = 0.66 fiber with a tapered region length of 1 m, simulated sweeping the signal wavelength from 1.4 μm to 2.8 μm is plotted. To better compare with the experimental results on FUT2, we considered a coupled pump power of 50 mW in the tapered region. As it is shown in Fig. 7, pumping in the anomalous dispersion region, very close to the ZDW point, at 1964 nm, will lead to a very broad conversion bandwidth, of about 200 nm at 3 dB, around the pump wavelength. Then, by tuning the pump wavelength by only 11 nm in the normal region, to 1953 nm, because of the high dispersive nature of the tapered fiber, we observe a strong reduction of the conversion bandwidth, down to 60 nm, near the pump wavelength. However, thanks to the high order contribution of the dispersion (see Eq. (1) [22]), from the simulation β_4 is expected to be negative before 2.134 μm, we would expect idler wave generation in the Mid-IR at about 2.643 μm by employing a telecom band signal laser, as shown in Fig. 7. At these pump wavelengths, the theoretical effective area is $1.7 \cdot 10^{-12}$ m^2, and employing the measured value for the nonlinear refractive index, the calculated nonlinear parameter is γ = 9.8 W^{-1}m^{-1}, almost 6 times larger than FUT2. A maximum CE ~-6 dB is found for both pumping wavelengths, however, the actual conversion efficiency is expected to be lower due to the linear loss of tapered ChG PCF.

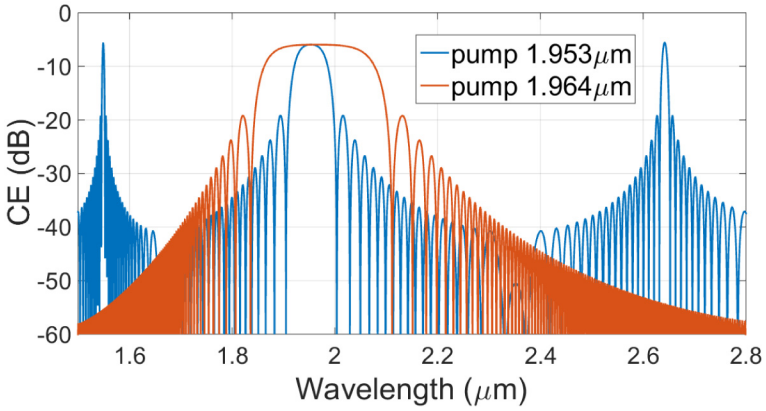

Fig. 7. The simulated CE plot with pump wavelengths at 1.964 μm and 1953 μm.

#259937 Received 26 Feb 2016; revised 30 Mar 2016; accepted 31 Mar 2016; published 26 Apr 2016

5. Conclusions

We have experimentally shown CW FWM in two different ChG PCFs in the 2 μm wavelength region. The signal and the pump lasers were two custom made CW tunable Thulium fiber lasers requiring only off-the shelf telecommunication components to operate. The first fiber under test (FUT1) was an AsSe PCF, with a core diameter of 14 μm. The measured dispersion $D = -336$ ps/nm/km at 1981 nm fits well with the simulations (about 0.6% error). We obtained a Kerr index of $n_2 \approx 7.9 \cdot 10^{-14}$ cm^2/W, comparable with the results found in literature at telecommunication wavelengths. Thanks to the high material nonlinearity, a maximum conversion efficiency of −36 dB with 150 mW of coupled pump power was measured despite the large normal dispersion. The second fiber we tested (FUT2) was a GeAsSe PCF with a core diameter of 4 μm and a shorter ZDW. We retrieved the dispersion by FWM for three different pump wavelengths, obtaining a 3dB conversion bandwidth of 24 nm at 2008 nm. A nonlinear parameter $\gamma \approx 1.688$ W^{-1}m^{-1} was derived from the measurement, allowing conversion efficiency per unit length and coupled pump power more than one order of magnitude larger than FUT1. The Kerr index at two micron was estimated to be $n_2 \approx 5.3 \cdot 10^{-14}$ cm^2/W. In the last part, building up from our experimental results, we have proposed a new fiber design based on a tapered GeAsSe PCF with a core diameter of 1.5 μm and a diameter-to-pitch ratio of 0.66. Both of these values can be achieved by using state of the art techniques in the ChG fiber fabrication. We have shown, in this configuration, a ZDW at 1963.4 nm leading to a $\gamma \approx 9.8$ W^{-1}m^{-1}. By slightly tuning the pump wavelength, either a large 3 dB conversion bandwidth of 200 nm around the pump or idler generation at even longer wavelength in the MIR by using telecom band signal lasers is possible. In conclusion, we believe that ChG PCFs are a promising approach to get efficient wavelength conversion in the SWIR or MIR region. Small core diameters with high nonlinear coefficients and ZDW around two micron are possible, maintaining the advantages that photonic crystal fibers have over waveguides based on air guided modes, like suspended core structures and integrated waveguides. In fact, tapered ChG PCFs still exhibit a fixed number of guided modes over an extended wavelength region, low propagation losses and degradation, allowing long interaction length with thicker and more robust structures.

Acknowledgments

We thank PERFOS for fabricating the ChG fibers, now commercially available from SelenOptics (www.selenoptics.com). We thank Arnaud Mussot and the University of Lille for the 2008 nm FBG fabrication. This work was supported by the European Research Council under grant agreement ERC-2012-StG 306630-MATISSE.

#259937 Received 26 Feb 2016; revised 30 Mar 2016; accepted 31 Mar 2016; published 26 Apr 2016